

# A Perceptual Distortion Reduction Framework for Adversarial Perturbation Generation

Ruijie Yang<sup>1</sup>, Yunhong Wang<sup>1</sup>, Yuanfang Guo<sup>1</sup>

<sup>1</sup> School of Computer Science and Engineering, Beihang University, China

## Abstract

Most of the adversarial attack methods suffer from large perceptual distortions such as visible artifacts, when the attack strength is relatively high. These perceptual distortions contain a certain portion which contributes less to the attack success rate. This portion of distortions, which is induced by unnecessary modifications and lack of proper perceptual distortion constraint, is the target of the proposed framework. In this paper, we propose a perceptual distortion reduction framework to tackle this problem from two perspectives. We guide the perturbation addition process to reduce unnecessary modifications by proposing an activated region transfer attention mask, which intends to transfer the activated regions of the target model from the correct prediction to incorrect ones. Note that an ensemble model is adopted to predict the activated regions of the unseen models in the black-box setting of our framework. Besides, we propose a perceptual distortion constraint and add it into the objective function of adversarial attack to jointly optimize the perceptual distortions and attack success rate. Extensive experiments have verified the effectiveness of our framework on several baseline methods.

## 1 Introduction

Deep Neural Networks (DNNs) have achieved tremendous success in various vision tasks, such as image classification, object detection, etc. Unfortunately, these DNNs, which are recently observed to be easily fooled by a special kind of small perturbations to give false outputs, are surprisingly vulnerable [Heaven, 2019]. This type of small perturbations, named adversarial perturbations [Szegedy *et al.*, 2014], is usually specifically generated by the adversary and added to the inputs of the DNNs to generate certain modified inputs, i.e., the adversarial examples, to attack the DNNs. Numerous researches [Goodfellow *et al.*, 2015; Kurakin *et al.*, 2017; Madry *et al.*, 2018; Carlini and Wagner, 2017; Zheng *et al.*, 2019] have been subsequently conducted on the adversarial attacks to investigate and understand the vulnerabilities and

the mechanisms of DNNs. Then, researchers can develop DNNs with more robustness and precise explanations.

Typical adversarial examples, which are generated by typical adversarial attack techniques, tend to possess obvious perceptual distortions, as shown in Fig. 1, when a high attack success rate (ASR) is demanded. These obvious perceptual distortions are easily to be spotted by human perceptions, which prevents the adversarial examples from being eliminated. We believe that a portion of these perceptual distortions are mainly induced by unnecessary modifications and lack of proper constraint.

The existing adversarial attack methods usually treat all the pixels in the input image equally. However, different pixels in an image tend to contribute differently to the output of the DNNs [Selvaraju *et al.*, 2020]. Therefore, the modifications to certain pixels, which actually contribute less to the attack success rate of targeted/non-targeted attacks, may be unnecessary.

Most of the existing adversarial attack methods assume the modifications on inputs are constrained by a  $L_p$  ball. Typically, it can be formulated as  $\|x_{adv} - x\|_p < \epsilon$ , where  $x_{adv}$  and  $x$  represent the perturbed and original inputs, respectively, and  $\epsilon$  is a predefined small constant which controls the maximum distance between  $x_{adv}$  and  $x$ . As mentioned in literatures [Zhang *et al.*, 2011], the  $L_p$  ball constraint is inconsistent with human visual perception.

Currently, there exists several literatures [Dong *et al.*, 2020a; Göpfert *et al.*, 2020; Deng and Karam, 2020; Wang *et al.*, 2020], which alleviate the distortions from different perspectives. [Dong *et al.*, 2020a] focuses on adding the perturbations only to the activated regions of the target model, which ignores the potentials of the other pixels. Meanwhile, [Göpfert *et al.*, 2020; Deng and Karam, 2020; Wang *et al.*, 2020] only constrain the perturbations by adaptively thresholding them in spatial/frequency domains, according to certain criteria such as just noticeable difference (JND), etc. They, as well as the other adversarial attack methods, have not explicitly considered the tradeoff between the attack success rate and the perceptual distortions.

In this paper, we focus on reducing the perceptual distortions in the adversarial examples while maintaining a high attack success rate. By considering the trade-off between the attacking ability and the perceptual distortions, we propose a perceptual distortion reduction (PDR) framework for ad-

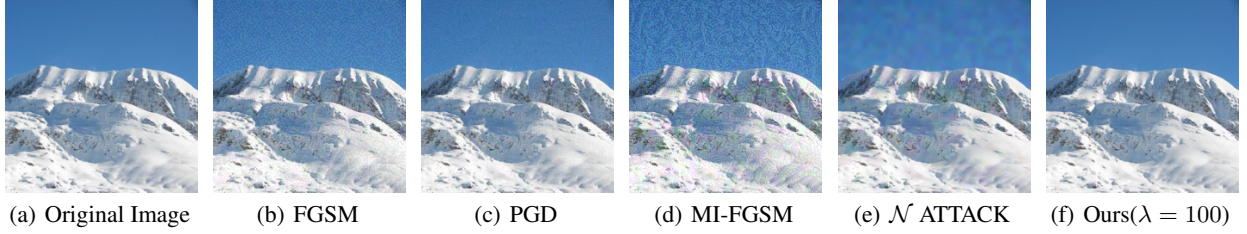


Figure 1: The adversarial examples. (a) is the original image and (b)~(f) are the adversarial examples generated by different methods. The original image (a) is correctly classified by ResNet50. (b)~(f) are misclassified. From the generated adversarial examples, we can observe that the popular adversarial attack methods tend to induce obvious visible artifacts, regardless of white-box attacks or black-box attacks. On the contrary, by applying our framework to a baseline adversarial attack method, the improved method(PGD-PDR) can generate adversarial examples which are visually pleasing.

versarial perturbation generation, to reduce the visible artifacts. Specifically, we reduce the unnecessary modifications by constructing an activated region transfer based attention (ARTA) module. The module predicts the most and least activated regions of the target model, which give significant responses to the correct and certain incorrect classes, respectively, and then generates a corresponding mask to constrain the perturbations to transfer the activated regions to achieve the attack. Besides, we propose a perceptual distortion regularization term in the final objective function with a Lagrangian multiplier  $\lambda$  to model the tradeoff between the attack success rate and perceptual distortions. By utilizing the proposed framework, our method can still preserve a decent attack success rate, with an obvious perceptual distortion reduction. For convenience, the image classification task is employed as a demonstration of our framework in this paper, while our framework can be applied to many tasks, such as object detection, segmentation and etc.

Our contributions are summarized as follows:

- We propose a perceptual distortion reduction framework, which can be applied to iterative adversarial perturbation generation methods, to explicitly model the tradeoff between the perceptual distortions and attack success rate.
- We propose to reduce the unnecessary modifications, by constraining the modification regions with a mask, which is predicted by exploiting a proposed activated region transfer mechanism.
- We propose to utilize the ensemble model to predict the common network activated regions in the black-box setting of our PDR framework.
- We propose to add a perceptual distortion constraint into the objective function, to reduce the perceptual distortions while maintaining a high attack success rate.

## 2 Related Work

In this section, we will review the literatures of adversarial attack and perceptual distortion evaluation.

### 2.1 Adversarial Attack

According to the adversary’s knowledge, adversarial attacks can be classified into two categories, the white-box and

black-box attacks. White-box attacks usually assume that the adversary can access all the information of the target model, including model architecture, parameters, training data and etc. For the black-box attacks, the adversary possesses limited/none information about the target model.

**White-box Attacks:** Most of the white-box attack techniques generate the adversarial examples based on the gradients of the loss function to inputs. The fast gradient sign method (FGSM) [Goodfellow *et al.*, 2015] is proposed as an one step method, which adds a maximum perturbation to the inputs in the direction that increases the distance between the adversarial example and the target class label. Basic iterative method (BIM) [Kurakin *et al.*, 2017] extends FGSM by iteratively adjusting the direction of the perturbation addition and adding multiple small perturbations. Similar to BIM, projected gradient descent (PGD) [Madry *et al.*, 2018] introduces a random perturbation addition step to pre-process the inputs to acquire a larger attack strength. Carlini & Wagner’s method [Carlini and Wagner, 2017] modifies the traditional loss function and transforms the inputs with the  $\arctanh(\cdot)$  transformation on inputs for the convenience of optimization. DAA [Zheng *et al.*, 2019] obtains an optimal adversarial-data distribution which satisfies the  $L_\infty$  constraint to produce adversarial examples.

**Black-box Attacks:** Based on the knowledge of the model, black-box attack schemes can be further categorized into transfer-based, score-based and decision-based attacks [Dong *et al.*, 2020b]. Transfer-based attacks assume that the adversary only possess the training data of the model and utilize a substitute model to generate adversarial examples which can fool the unseen models because the adversarial examples possess certain transferability [Dong *et al.*, 2018; Dong *et al.*, 2019; Zou *et al.*, 2020]. Score-based attacks assume that the adversary can acquire the output probabilities by querying the target model [Chen *et al.*, 2017; Ilyas *et al.*, 2018; Li *et al.*, 2019]. Decision-based attack approaches only know the hard label predictions (without probabilities) of the target model [Brendel *et al.*, 2018; Cheng *et al.*, 2019; Shi *et al.*, 2020].

Both the white-box and black-box attack techniques have been developed rapidly in recent year. Unfortunately, most of the methods have not paid enough attention to minimizing the perceptual distortions. They tend to generate adversarial examples with obvious visible artifacts when a high

attack success rate is demanded. Some recent efforts have been made to reduce the perceptual distortions. [Göpfert *et al.*, 2020] adopts adaptive thresholds to add the perturbations to different image pixels with different local complexities. [Deng and Karam, 2020] utilizes the just noticeable difference (JND) thresholds in the discrete cosine transform (DCT) based frequency domain to constrain the addition of adversarial perturbations. [Wang *et al.*, 2020] applies spatial and frequency JND models to estimate the maximal adversarial perturbation bounds in the two domains separately and predicts two thresholds to accordingly construct two adversarial attack methods. Different from the existing JND based adversarial approaches, we are constructing a perceptual distortion reduction framework by reducing the unnecessary modifications on the less important pixels and constraining the perceptual distortion in the objective function.

## 2.2 Perceptual Distortion Evaluation

In adversarial attacks, the basic image distortion measurement is the  $L_p$  distance, which is easy to calculate and convenient to apply. However, this distortion measure, which is similar to the conventional metrics such as peak signal-to-noise ratio (PSNR) and mean-squared error (MSE), does not match human visual system (HVS) well. In the past two decades, a large number of image quality assessment metrics, which were designed based on human perception mechanisms, have been proposed in literatures. The famous structure similarity (SSIM) Index [Wang *et al.*, 2004] is developed based on the hypothesis that HVS is highly sensitive to the structural information in images. Subsequently, feature similarity (FSIM) index [Zhang *et al.*, 2011] assumes that phase congruency is the primary feature in HVS. Recently, deep neural networks have also been adopted to evaluate the perceptual distortions in images [Zhang *et al.*, 2018; Kim *et al.*, 2020].

There exist many perceptual distortion evaluation methods which can behave decently in simulating the human visual system. We can adopt these methods to evaluate the perceptual distortions of the generated adversarial perturbations.

## 3 Proposed Work

In this section, we firstly define the notations employed here. Then, our proposed framework will be presented.

### 3.1 Notations

Let  $x$  be the original input. Let  $y$  be the ground-truth label. A classification DNN can be represented as  $C_\theta : X^{C \times W \times H} \rightarrow Y^n$ , where  $X$  stands for the input space with dimension  $Channel \times Width \times Height$ ,  $Y$  denotes the classification space with  $n$  categories, and  $\theta$  is the parameters of  $C$ . The output of the classification network is represented as  $C_\theta(x) = (c_1, c_2, \dots, c_i, \dots, c_n)$ , where  $c_i$  is the confidence score for class  $i$  and  $n$  is the number of classes.

For an ideal DNN model, we can assume that the network will give a correct prediction on image  $x$ , i.e.,  $\underset{1 \leq i \leq n}{\operatorname{argmax}} C_\theta(x) = y$ .

For a real model, this assumption tends to hold only for most of the clean samples. When an adversarial example  $x_{adv}$

is generated by an attack method  $F(\cdot)$  and fed into the classification model,  $C_\theta$ , the adversarial example  $x_{adv}$  tends to be misclassified. This misclassification process can be represented as  $x_{adv} = F(x, C_\theta)$  such that  $\underset{1 \leq i \leq n}{\operatorname{argmax}} C_\theta(x_{adv}) \neq y$ .

Note that  $x_{adv}$  is usually desired to be visually similar to  $x$ . Most of the adversarial attack methods constrain  $x_{adv}$  to satisfy  $\|x_{adv} - x\|_p < \epsilon$ , where  $\epsilon$  is a small constant. Note that the norm  $\|\cdot\|_p$  employs  $p = \infty$ ,  $p = 2$  or  $p = 0$ .

### 3.2 Overall Framework

Current adversarial perturbation generation methods usually focus on achieving a high attack success rate. Meanwhile, they also generate visible artifacts in the adversarial examples. The perceptual distortions in typical adversarial examples are mainly induced by the lack of proper constraint for perceptual distortions and the unnecessary modifications to the unimportant pixels/regions. To effectively reduce the perceptual distortions in the adversarial examples while preserving a decent attack strength, we propose a perceptual distortion reduction (PDR) framework, which is illustrated in Fig. 2. Specifically, after data pre-processing, the input original image will be processed by an iterative adversarial perturbation generation module to generate the initial adversarial perturbations. To reduce the unnecessary modifications induced by considering all the pixels equally, we construct an activated region transfer based attention (ARTA) module, which generates an attention mask by calculating the most and least activated regions of the target model in the input images. The attention mask is then utilized in the fusion module to revise the initial perturbations, and the revised perturbations will be added to the original image to construct the adversarial image  $x_{adv}^j$ , which can be formulated as  $x_{adv}^j = x + P * S$ . To further reduce the visible artifacts, we propose to add an perceptual distortion constraint to the final objective function of the adversarial perturbation generation stage, to jointly optimize the attack success rate and the visual quality of the examples.

### 3.3 Activated Region Transfer based Attention Module

Currently, most of the adversarial attack methods treat all the pixels in the original image equally. This strategy has not taken the divergences of the pixels into consideration during the generation process of adversarial perturbations. On the contrary, the DNNs tend to give different responses to different pixels in the input image. When an image is classified to a specific category, the major responses will be concentrated to certain regions [Selvaraju *et al.*, 2020]. Therefore, the traditional strategy, which equally modifies all the pixels in the original image, tends to introduce unnecessary distortions at the regions where the DNN pays less attention to. These unnecessary distortions can be reduced by adaptively adding the adversarial perturbations to certain regions, rather than the entire image, such that the attack strength is preserved.

To induce a misclassification, where an adversarial example  $x_{adv}$  is expected to be classified to another class  $\tilde{y}$ , an intuitive solution is to manipulate the original activated region of the target model for class  $y$  by adding certain pertur-

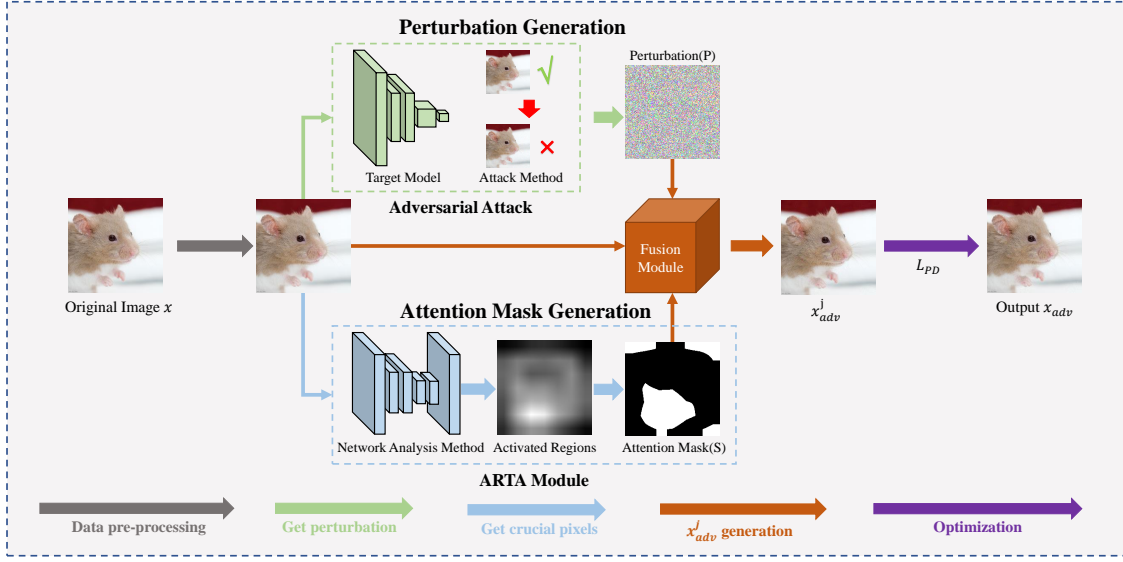


Figure 2: The proposed perceptual distortion reduction framework. Firstly, an adversarial attack method is selected to generate the initial adversarial perturbation (P). Then, the ARTA module is exploited to predict the most and least activated regions of the target model and generate an attention mask S to revise the perturbation addition process by transferring the activated regions of the target model. In the fusion module, we generate the revised adversarial perturbation via  $x_{adv}^j = x + P * S$ . Note that a perceptual distortion constraint  $L_{PD}$  is added to the objective function to constrain the distortions to be more human perception friendly. At last, the adversarial example is gradually optimized and we can obtain a visually pleasing adversarial example  $x_{adv}$ .

bations to image  $x$ . Different from the existing work [Dong *et al.*, 2020a], which only adds the perturbations to the most activated region of the target model for class  $y$ , we intend to simultaneously add perturbations to the activated regions for class  $y$  and  $\tilde{y}$ , such that the activated regions of the target model can be transferred to give high responses to the regions highly corresponding to class  $\tilde{y}$ . If the adversarial attack is a non-targeted attack, we utilize the least activated region for class  $y$ , which is highly likely to be corresponding to the other categories, as a substitute. In our ARTA module, we firstly obtain the network attention map  $M$ , whose value represents the response of the target model at each pixel location, via an network analysis method  $AM(\cdot)$ , as

$$M = AM(x, C_\theta). \quad (1)$$

Then, we apply a mapping  $T(\cdot)$  to  $M$  to obtain an attention mask  $S$ , which highlights the most and least activated region for class  $y$ , as

$$S = T(M), \quad (2)$$

where  $T(\cdot)$  denotes the mapping operation. Intuitively, this mapping can be achieved via any reasonable functions. For convenience, we simply employ  $T(M) = (M > t_{high}) + (M < t_{low})$ , where  $t_{high}$  and  $t_{low}$  are thresholds for predicting the most focused region and least activated regions, in this paper.

Note that the Grad-CAM [Selvaraju *et al.*, 2020] is exploited to serve as the DNN analysis method  $AM(\cdot)$  in Eq. 1, to predict the mask. Besides, if the proposed PDR framework is applied to a black-box adversarial attack, the target model cannot be directly analyzed to predict the activated regions. Under such circumstances, we utilize multiple standard mod-

els  $\{C_\theta^1, C_\theta^2, \dots, C_\theta^k\}$  to ensemble a substitute model to estimate the activated region  $M$  of the target model, via

$$M = \frac{1}{k} (AM(x, C_\theta^1) + AM(x, C_\theta^2) + \dots + AM(x, C_\theta^k)) \quad (3)$$

Then, the estimated  $M$  can be adopted in Eq. 2 for subsequent processing steps.

### 3.4 Perceptual Distortion Constrained Objective Function

The existing adversarial attack methods usually constrain the perturbation with a  $L_p$  ball by clipping the excessive perturbations to the maximal allowed value. Unfortunately, the  $L_p$  distance is inconsistent with human visual system, and the generated adversarial examples tend to contain obvious visible artifacts when the attack strength is high.

To effectively reduce the perceptual distortions, we propose to add a perceptual distortion constraint  $L_{PD}$  to the final objective function. However, since the allowed range of the distortions is usually inversely proportional to the attack success rate, the perceptual distortion constraint may not be suitable to be directly added to the objective function. Therefore, we model the tradeoff between the perceptual distortions and the attack strength via an Lagrangian multiplier  $\lambda$ , which can be utilized to control the balance between the perceptual distortions and attack strength. By maintaining the optimization term for misclassification  $L_{mis}$ , the final objective function can be formulated as

$$L_{total}(x_{adv}; x, C_\theta) = L_{mis}(x_{adv}, C_\theta) + \lambda L_{PD}(x, x_{adv}). \quad (4)$$

Note that the typical optimization algorithms for the adversarial perturbation generation methods can be easily applied

---

**Algorithm 1** The PDR Framework

---

**Input:** image  $x$ , label  $y$ , target network  $C_\theta(\cdot)$ , adversarial attack method  $F(\cdot)$ , network analysis method  $AM(\cdot)$ , perceptual distortion constraint  $L_{PD}$

**Parameter:**  $\lambda, \kappa, t_{high}, t_{low}$

**Output:** adversarial example  $x_{adv}$

```

1: Use  $L_{total} = L_{mis} + \lambda L_{PD}$  to replace the objective function in  $F(\cdot)$ 
2:  $M = AM(x, C_\theta)$ 
3:  $S = (M > t_{high}) + (M < t_{low})$ 
4:  $x_{adv}^0 = x$ 
5: Let  $j = 1$ .
6: while True do
7:    $x_{adv}^j = F(x_{adv}^{j-1}, C_\theta)$ 
8:    $x_{adv}^j = x + S \cdot (x_{adv}^j - x)$ 
9:   if  $x_{adv}^j$  satisfies the termination condition of  $F(\cdot)$  then
10:    Break
11:  end if
12: end while
13: return  $x_{adv} = x_{adv}^j$ 

```

---

to solve Eq. 4 and the  $L_{mis}$  and  $L_{PD}$  terms in Eq. 4 can both adopt any reasonable models. For convenience, in this paper, we choose the function  $f_6$  in [Carlini and Wagner, 2017] as  $L_{mis}$ , which is defined as

$$L_{mis}(x', C_\theta) = \max(\max(Z(x')_i : i \neq y) - Z(x')_y, -\kappa), \quad (5)$$

where  $\kappa$  is a parameter to control the strength of the adversarial examples. Similarly, the proposed perceptual distortion constraint  $L_{PD}$  adopts the popular perceptual distortion evaluation metric  $SSIM$ , which is defined as

$$L_{PD}(x, x') = SSIM(x, x') = \frac{(2\mu_x\mu_{x'} + K_1)(2\sigma_{x,x'} + K_2)}{(\mu_x^2 + \mu_{x'}^2 + K_1)(\sigma_x^2 + \sigma_{x'}^2 + K_2)}, \quad (6)$$

where  $\mu_x, \sigma_x$  are the mean and variance of image  $x$ , respectively, and  $\sigma_{x,x'}$  represents the covariance between  $x$  and

$x'$ , i.e.,  $\mu_x = \frac{1}{N} \sum_{i=1}^N x_i$ ,  $\sigma_x = (\frac{1}{N-1} \sum_{i=1}^N (x_i - \mu_x)^2)^{\frac{1}{2}}$  and

$\sigma_{x,x'} = \frac{1}{N-1} \sum_{i=1}^N (x_i - \mu_x)(x'_i - \mu_{x'})$ . We choose  $K_1 = 0.01$  and  $K_2 = 0.03$  by following the original settings and implementations in [Wang *et al.*, 2004].

## 4 Experiments

In this section, the proposed PDR framework will be applied to several popular adversarial attack methods, where the improved method is named as X-PDR, for both the black-box and white-box settings, to evaluate the effectiveness of the proposed work.

### 4.1 Setups

In the experiments, the ImageNet dataset [Deng *et al.*, 2009] is employed for both the black-box and white-box attacks. We randomly select the 1000 images from the validation set of the ImageNet dataset to generate adversarial

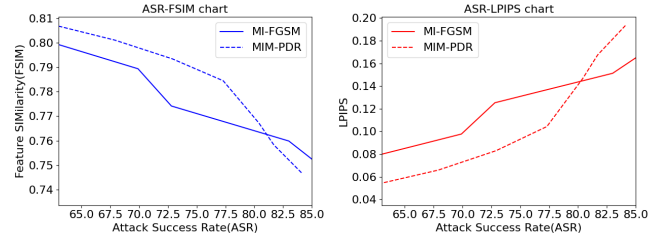


Figure 3: The results when MI-FGSM is employed as the baseline.

examples. Since our framework can be applied to arbitrary iterative adversarial perturbation generation methods, we select the most popular methods for better demonstration. For black-box attacks, MI-FGSM [Dong *et al.*, 2018] and  $\mathcal{N}$  ATTACK [Li *et al.*, 2019] are utilized. In MI-FGSM, the pre-trained ResNet-101, Inception-v3 and DenseNet-161 are employed to form an ensemble network as the substitute model to generate the adversarial examples. In black-box attacks, we also utilize this ensemble model to predict the activated region of the target model. Since MI-FGSM can be easily applied to the white-box attacks, MI-FGSM and PGD [Madry *et al.*, 2018] are employed. We set parameters  $\kappa = 50$ . We set  $t_{high} = \{t \mid p(R \geq t) = 0.25\}$  and  $t_{low} = \{t \mid p(R \leq t) = 0.25\}$ . Other parameters are set the same as that in the original papers.

For better comparison, we calculate the attack success rate and perceptual distortion metrics to measure the performance of each method. The attack success rate (ASR) is defined as:

$$ASR = 1 - \frac{\#\{\text{correct samples}\}}{\#\{\text{total samples}\}}. \quad (7)$$

We choose the popular traditional metric FSIM [Zhang *et al.*, 2011] and deep metric LPIPS [Zhang *et al.*, 2018] to evaluate the perceptual distortion.

### 4.2 Results

**Black-box Results:** For black-box attacks, MI-FGSM attack and  $\mathcal{N}$  ATTACK are employed as our baselines. Note that the modified MI-FGSM is named MIM-PDR for convenience. Due to limited space, the results of  $\mathcal{N}$  ATTACK are presented in the supplementary materials.

Since MI-FGSM has already considered to evaluate attack methods on the unseen models, VGG-16, ResNet-50 and MobileNet-v2. The results are shown in Table 1. As can be observed, the attack success rate declines while the perceptual quality increases, which verifies the tradeoff between them. Besides, when  $\lambda$  increases, the perceptual quality constraint becomes more important in the objective function, thus the accordingly generated adversarial examples will have better perceptual quality yet with a slightly decreased ASR. For better illustration, we draw a figure of attack success rate versus perceptual distortion, as shown in Fig. 3. Fig. 3 demonstrates that our method MIM-RPD achieves the best performance when the allowed perceptual distortions are relatively small. With the same perceptual distortion level, our method can get the highest attack success rate. Note that our method



Attack Method	VGG-16	ResNet-50	MobileNet-v2	FSIM	LPIPS
MI-FGSM( $\epsilon=16$ )	85.6	96.6	88.5	0.6575	0.3341
MI-FGSM( $\epsilon=12$ )	80.0	94.4	85.2	0.6940	0.2722
MI-FGSM( $\epsilon=8$ )	68.6	89.2	76.1	0.7371	0.1932
MI-FGSM( $\epsilon=4$ )	49.7	70.0	55.7	0.7893	0.0977
MIM-PDR( $\lambda = 40$ )	63.2	82.7	75.2	0.7583	0.1675
MIM-PDR( $\lambda = 100$ )	61.7	80.4	68.2	0.7672	0.1446
MIM-PDR( $\lambda = 500$ )	55.6	72.9	60.0	0.7934	0.0830
MIM-PDR( $\lambda = 1200$ )	47.7	62.8	50.1	0.8069	0.0539

Table 1: Results when the black-box MI-FGSM is employed as the baseline. The numbers in columns 2-5 represent the ASR(%). The results of FSIM and LPIPS are obtained by computing average result for all the samples.

Attack method	ResNet-50	FSIM	LPIPS
PGD	100.0	0.7537	0.1273
PGD-PDR( $\lambda = 40$ )	99.7	0.8393	0.0184
PGD-PDR( $\lambda = 100$ )	99.4	0.8402	0.0158
PGD-PDR( $\lambda = 1200$ )	94.5	0.8456	0.0059
MI-FGSM	100.0	0.6592	0.3457
MIM-PDR( $\lambda = 40$ )	98.8	0.7536	0.1902
MIM-PDR( $\lambda = 100$ )	98.4	0.7593	0.1754
MIM-PDR( $\lambda = 1200$ )	95.1	0.7984	0.0743

Table 2: The results when PGD and white-box MI-FGSM are employed as the baselines. Column 2 is the ASR(%) results. The results of FSIM and LPIPS are obtained by computing the average results of all the samples.

gives a slightly worse ASR when very large perceptual distortions are allowed, because our method only modifies certain regions in the images, which hampers the transferability of the adversarial examples compared to the modifications to the entire image. Since the generated adversarial examples with very large perturbations usually contain obvious visible artifacts, they are easily being spotted by the users.

**White-box Results:** For white-box attacks, PGD and MI-FGSM attack are employed as the baselines. The results are summarized in Table 2. As can be observed from Table 2, all the methods can achieve very good attack success rate ( $> 94\%$ ). Although the attack success rate has slightly dropped in our methods, we can significantly improve the visual quality of the adversarial examples (images). An intuitive comparison is given in Fig. 1. As can be observed, by applying our PDR framework, the result of PGD-PDR contains none visible artifacts.

### 4.3 Discussion

**How the target model is affected by our method:** Many literatures have concluded that DNNs usually focus on certain region in an image during classification. Here, we visualize the network activated maps of the original image and adversarial example separately, to verify the effectiveness of our activated region transfer mechanism. Note that the target model employed here is ResNet-50 and the adversarial attack baseline method is PGD-PDR. For fair comparison, instead of directly normalizing the dynamic range of the maps to  $[0, 1]$ , the same normalization ratio is employed. Fig. 4 shows the result. As can be observed, before adding the perturbations to the inputs, the target network gives major responses to the

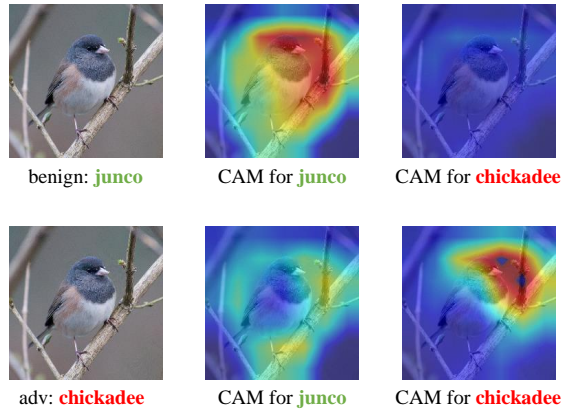


Figure 4: Visualization of the activated regions before and after adversarial attack. Grad-CAM is used for predicting the activated regions and target model is ResNet-50. The second column shows the CAM results for the correct class junco while the third column shows the CAM results for the adversarial class chickadee.

region of class junco. After the perturbations are added, the responses at the regions corresponding to the original class junco have been reduced and the responses at the regions corresponding to another class chickadee is obviously increased. This phenomenon verifies the effectiveness of our activated region transfer mechanism.

## 5 Conclusion

In this paper, we propose a perceptual distortion reduction framework to alleviate the obvious visible artifacts in the adversarial examples. The proposed framework can be easily applied to typical iterative adversarial perturbation generation methods. We reduce the unnecessary modifications in the adversarial examples by proposing an activated region transfer mechanism and guiding the perturbation generation with a predicted mask. For the black-box setting of our proposed framework, we utilize an ensemble model to predict the attention mask. Different from previous approaches, which usually constrain adversarial examples within an  $L_p$  ball, we introduce a new perceptual distortion constraint  $L_{PD}$  to the objective function of the adversarial attack and thus achieve a joint optimization of the attack success rate and perceptual distortion. Extensive experiments have demonstrated the effectiveness of our proposed PDR framework.

## References

- [Brendel *et al.*, 2018] Wieland Brendel, Jonas Rauber, and Matthias Bethge. Decision-based adversarial attacks: Reliable attacks against black-box machine learning models. In *ICLR*, 2018.
- [Carlini and Wagner, 2017] Nicholas Carlini and David A. Wagner. Towards evaluating the robustness of neural networks. In *IEEE S & P*, pages 39–57, 2017.
- [Chen *et al.*, 2017] Pin-Yu Chen, Huan Zhang, Yash Sharma, Jinfeng Yi, and Cho-Jui Hsieh. Zoo: Zeroth order optimization based black-box attacks to deep neural networks without training substitute models. In *WAIS*, pages 15–26, 2017.
- [Cheng *et al.*, 2019] Minhao Cheng, Thong Le, Pin-Yu Chen, Huan Zhang, Jinfeng Yi, and Cho-Jui Hsieh. Query-efficient hard-label black-box attack: An optimization-based approach. In *ICLR*, 2019.
- [Deng and Karam, 2020] Yingpeng Deng and Lina J. Karam. Frequency-tuned universal adversarial attacks. *CoRR*, abs/2003.05549, 2020.
- [Deng *et al.*, 2009] Jia Deng, Wei Dong, Richard Socher, Li-Jia Li, Kai Li, and Li Fei-Fei. Imagenet: A large-scale hierarchical image database. In *IEEE Conference on Computer Vision and Pattern Recognition*, pages 248–255, 2009.
- [Dong *et al.*, 2018] Yinpeng Dong, Fangzhou Liao, Tianyu Pang, Hang Su, Jun Zhu, Xiaolin Hu, and Jianguo Li. Boosting adversarial attacks with momentum. In *IEEE CVPR*, pages 9185–9193, 2018.
- [Dong *et al.*, 2019] Yinpeng Dong, Tianyu Pang, Hang Su, and Jun Zhu. Evading defenses to transferable adversarial examples by translation-invariant attacks. In *IEEE CVPR*, pages 4312–4321, 2019.
- [Dong *et al.*, 2020a] Xiaoyi Dong, Jiangfan Han, Dongdong Chen, Jiayang Liu, Huanyu Bian, Zehua Ma, Hongsheng Li, Xiaogang Wang, Weiming Zhang, and Nenghai Yu. Robust superpixel-guided attentional adversarial attack. In *IEEE/CVF CVPR*, pages 12892–12901, 2020.
- [Dong *et al.*, 2020b] Yinpeng Dong, Qi-An Fu, Xiao Yang, Tianyu Pang, Hang Su, Zihao Xiao, and Jun Zhu. Benchmarking adversarial robustness on image classification. In *IEEE/CVF CVPR*, pages 318–328, 2020.
- [Goodfellow *et al.*, 2015] Ian J. Goodfellow, Jonathon Shlens, and Christian Szegedy. Explaining and harnessing adversarial examples. In *ICLR*, 2015.
- [Göpfert *et al.*, 2020] Jan Philip Göpfert, André Artelt, Heiko Wersing, and Barbara Hammer. Adversarial attacks hidden in plain sight. In *IDA*, pages 235–247, 2020.
- [Heaven, 2019] Douglas Heaven. Why deep-learning aIs as easy to fool. *Nature*, 574:163–166, 2019.
- [Ilyas *et al.*, 2018] Andrew Ilyas, Logan Engstrom, Anish Athalye, and Jessy Lin. Black-box adversarial attacks with limited queries and information. In *ICML*, 2018.
- [Kim *et al.*, 2020] Hak Gu Kim, Heoun-taek Lim, and Yong Man Ro. Deep virtual reality image quality assessment with human perception guider for omnidirectional image. *IEEE TCSVT*, 30(4):917–928, 2020.
- [Kurakin *et al.*, 2017] Alexey Kurakin, Ian J. Goodfellow, and Samy Bengio. Adversarial examples in the physical world. In *ICLR*, 2017.
- [Li *et al.*, 2019] Yandong Li, Lijun Li, Liqiang Wang, Tong Zhang, and Boqing Gong. Nattack: Learning the distributions of adversarial examples for an improved black-box attack on deep neural networks. In *ICML*, pages 3866–3876, 2019.
- [Madry *et al.*, 2018] Aleksander Madry, Aleksandar Makelov, Ludwig Schmidt, Dimitris Tsipras, and Adrian Vladu. Towards deep learning models resistant to adversarial attacks. In *ICLR*, 2018.
- [Selvaraju *et al.*, 2020] Ramprasaath R Selvaraju, Michael Cogswell, Abhishek Das, Ramakrishna Vedantam, Devi Parikh, and Dhruv Batra. Grad-cam: Visual explanations from deep networks via gradient-based localization. *IJCV*, 128(2):336–359, 2020.
- [Shi *et al.*, 2020] Yucheng Shi, Yahong Han, and Qi Tian. Polishing decision-based adversarial noise with a customized sampling. In *IEEE/CVF CVPR*, pages 1027–1035, 2020.
- [Szegedy *et al.*, 2014] Christian Szegedy, Wojciech Zaremba, Ilya Sutskever, Joan Bruna, Dumitru Erhan, Ian J. Goodfellow, and Rob Fergus. Intriguing properties of neural networks. In *ICLR*, 2014.
- [Wang *et al.*, 2004] Zhou Wang, Alan C. Bovik, Hamid R. Sheikh, and Eero P. Simoncelli. Image quality assessment: from error visibility to structural similarity. *IEEE TIP*, 13(4):600–612, 2004.
- [Wang *et al.*, 2020] Yongwei Wang, Mingquan Feng, Rabab Ward, Z. Jane Wang, and Lanjun Wang. Perception improvement for free: Exploring imperceptible black-box adversarial attacks on image classification. *CoRR*, abs/2011.05254, 2020.
- [Zhang *et al.*, 2011] Lin Zhang, Lei Zhang, Xuanqin Mou, and David Zhang. FSIM: A feature similarity index for image quality assessment. *IEEE TIP*, 20(8):2378–2386, 2011.
- [Zhang *et al.*, 2018] Richard Zhang, Phillip Isola, Alexei A. Efros, Eli Shechtman, and Oliver Wang. The unreasonable effectiveness of deep features as a perceptual metric. In *IEEE CVPR*, pages 586–595, 2018.
- [Zheng *et al.*, 2019] Tianhang Zheng, Changyou Chen, and Kui Ren. Distributionally adversarial attack. In *AAAI*, pages 2253–2260, 2019.
- [Zou *et al.*, 2020] Junhua Zou, Zhisong Pan, Junyang Qiu, Xin Liu, Ting Rui, and Wei Li. Improving the transferability of adversarial examples with resized-diverse-inputs, diversity-ensemble and region fitting. In *ECCV*, volume 12367, pages 563–579, 2020.